PROCEEDINGS B

rspb.royalsocietypublishing.org

Research

Cite this article: Prazeres M, Uthicke S, Pandolfi JM. 2015 Ocean acidification induces biochemical and morphological changes in the calcification process of large benthic foraminifera. *Proc. R. Soc. B* **282**: 20142782. http://dx.doi.org/10.1098/rspb.2014.2782

Received: 17 November 2014
Accepted: 14 January 2015

Subject Areas:
ecology, physiology

Keywords:
large benthic foraminifera, ocean acidification, calcification, Ca-ATPase

Author for correspondence:
Martina Prazeres
e-mail: m.prazeres@uq.edu.au

Electronic supplementary material is available at http://dx.doi.org/10.1098/rspb.2014.2782 or via http://rspb.royalsocietypublishing.org.

THE ROYAL SOCIETY PUBLISHING

Ocean acidification induces biochemical and morphological changes in the calcification process of large benthic foraminifera

Martina Prazeres[1], Sven Uthicke[2] and John M. Pandolfi[1]

[1]Australian Research Council (ARC) Centre of Excellence for Coral Reef Studies and School of Biological Sciences, The University of Queensland, St Lucia, Queensland 4072, Australia
[2]Australian Institute of Marine Science, PMB No. 3, Townsville, Queensland 4810, Australia

JMP, 0000-0003-3047-6694

Large benthic foraminifera are significant contributors to sediment formation on coral reefs, yet they are vulnerable to ocean acidification. Here, we assessed the biochemical and morphological impacts of acidification on the calcification of *Amphistegina lessonii* and *Marginopora vertebralis* exposed to different pH conditions. We measured growth rates (surface area and buoyant weight) and Ca-ATPase and Mg-ATPase activities and calculated shell density using micro-computer tomography images. In *A. lessonii*, we detected a significant decrease in buoyant weight, a reduction in the density of inner skeletal chambers, and an increase of Ca-ATPase and Mg-ATPase activities at pH 7.6 when compared with ambient conditions of pH 8.1. By contrast, *M. vertebralis* showed an inhibition in Mg-ATPase activity under lowered pH, with growth rate and skeletal density remaining constant. While *M. vertebralis* is considered to be more sensitive than *A. lessonii* owing to its high-Mg-calcite skeleton, it appears to be less affected by changes in pH, based on the parameters assessed in this study. We suggest difference in biochemical pathways of calcification as the main factor influencing response to changes in pH levels, and that *A. lessonii* and *M. vertebralis* have the ability to regulate biochemical functions to cope with short-term increases in acidity.

1. Introduction

Anthropogenic activities related to fossil fuel combustion over the last two centuries have led to an increase in atmospheric CO_2 partial pressure (pCO_2) levels from 280 ppm to about 400 ppm, which is around 40% higher than pre-industrial times [1]. According to the Intergovernmental Panel on Climate Change (IPCC), pCO_2 levels are likely to further increase and reach values between 650 and 1350 ppm by 2100 [2,3]. The rise of pCO_2 levels reduces seawater pH, a process known as ocean acidification (OA). This also causes a decline in calcium carbonate saturation state (Ω_{Cc}), mainly by reducing the concentration of carbonate ions in the seawater [4]. Based on the IPCC predictions [2], the decline in seawater pH is likely to range between 0.3 and 0.5 units by the end of this century, corresponding to a change in acidity of between 100 and 200%. For example, on the Great Barrier Reef, it is predicted that aragonite saturation state will drop to levels of approximately 2.4 by the end of the century [5], and in some inshore reef areas, pCO_2 has already risen to concentrations of approximately 450 ppm [6]. The effects of OA are likely to be widespread across a diversity of marine life [7]. The decline in calcite saturation state (Ω_{Ca}) results in reduced calcification and increased dissolution rates of major marine calcifiers such as corals, foraminifera, calcifying algae and some molluscs, with potentially severe implications for coral reef ecosystems [7,8–11]. However, there is a lack of sufficient understanding of calcification mechanisms to explain species-specific differences observed in manipulative

experiments [4,7,12]. Establishing the relationship between pCO_2 and calcification is important for assessing the impact of lowering pH in the future [13], and the possible ecological consequences for reef-dweller foraminiferal populations.

Foraminifera are important contributors to $CaCO_3$ (i.e. calcite and aragonite) cycling in the ocean [14,15] and are the most geographically widespread group of calcifying organisms, producing skeletons with either low-Mg or high-Mg calcite, depending upon taxa [16]. They are able to elevate pH at the site of calcification by at least one unit (i.e. an order of magnitude increase in H^+ ion concentrations) above seawater pH and, thereby overcome precipitation-inhibition at ambient Mg concentrations [16,17]. Among foraminifera species, photosymbiont-bearing large benthic foraminifera (LBF) species can contribute up to 80% of the global foraminiferal reef carbonate [14], approximately 1 kg $CaCO_3$ m^{-2} yr^{-1} [18]. Changes in pH are predicted to directly affect LBF survivorship over longer time frames by modifying shell structure, disrupting the calcification process and possibly causing severe symbiont loss, known as 'bleaching' [19,20]. As LBF rely on elevating the intracellular pH for their calcification [16,19], an ongoing and increasing extent of OA can result in a decrease of foraminiferal calcite production, as more energy needs to be spent by LBF to produce the same amount of calcite [16,21]. However, the presence of symbiotic algae was previously suggested to provide an advantage, as the increase in CO_2 concentration in the seawater releases the algae from dissolved inorganic carbon (DIC) limitation [17]. As a consequence, photosynthetic rates can be enhanced, resulting in an increase of pH levels within the foraminifera microenvironment [11,17].

The rate of calcification in LBF is highly affected by pH changes and decreases significantly when pH levels drop below 8.0 [22]. Several recent studies have explored the effects of OA on the growth, calcification and photobiology of LBF [10,11,23–26]. Decline in pH can decrease shell weight [24], cause reduction in calcification rates [10,11,24,26–28] and photosynthetic efficiency [27], and alter shell microfabric through dissolution of calcium carbonate crystals [25]. However, Vogel & Uthicke [23] showed either no effect or an increase in calcification rates of *Marginopora vertebralis* when exposed to pH lower than 7.6, and Uthicke & Fabricius [11] observed an initial increase in photosynthesis rates at low pH levels for this species. Local stressors such as exposure to elevated concentrations of dissolved inorganic nutrients can also act to lower the threshold of tolerance of LBF to changes in pH levels [26]. A recent meta-analysis on experimental data suggested that overall calcification in dinoflagellate-bearing high-Mg calcite foraminifera species are more sensitive to OA, whereas diatom-bearing low-Mg calcite counterparts tend to be more resistant to changes in pH conditions [29].

Little is known about the biochemical and physiological processes behind the response of LBF to lowered pH/increased pCO_2. To better understand these effects in foraminiferal biology, cellular diagnostic parameters, also known as biomarkers, have been developed to assess the cellular-physiological condition of LBF [30]. Biomarkers are key cellular parameters that link a specific environmental exposure to physiological or morphological alterations [31]. Use of biomarkers enables the identification of putative stressors, as well as the ability to forecast the biological effects of these stressors based on an understanding of cellular-level processes [30,31]. Recently, the use of micro-computer tomography (μCT-scan) has enabled a comprehensive, quantitative analysis of internal structures without specific preparation or destruction [32,33]. Here, we combine these two approaches (biochemical and morphological) to examine the response in the calcification process in LBF to future predicted levels of OA.

The main goals of this study were to determine the morphological and biochemical responses involved in growth and calcification of *Amphistegina lessonii* (d'Orbigny 1843) and *M. vertebralis* (Quoy and Gaimard 1830) to decreased pH/increased pCO_2 concentrations expected to occur within the next century and beyond. *Amphistegina lessonii* is mainly found attached to pieces of dead coral along the reef slope, at depths of more than 6 m [34], and *M. vertebralis* are abundant on the reef flat [35,36]. The two species differ in the chemical composition of their shells and symbiont type. *Amphistegina lessonii* precipitates low-Mg calcite and hosts diatoms, whereas shells of *M. vertebralis* consist of high-Mg calcite and host dinoflagellate endosymbionts. Besides differences in Mg content, *A. lessonii* also differs from *M. vertebralis* regarding calcification mechanism. *Amphistegina lessonii* is a calcareous, perforate species [19], while *M. vertebralis* produces porcelaneuos, imperforate skeleton [37]. Perforate species store calcium and carbonate in separate intracellular pools that are used to precipitate new chambers extracellularly, whereas imperforate individuals precipitate calcite intracellularly in vesicles, which are then transported to the calcification site [16]. Therefore, these species are likely to respond in different ways to changes in pH levels. Specifically, we measured growth rates (surface area and buoyant weight), and two enzymes known to be involved in the balance of intracellular Ca^{2+} and Mg^{2+} ions (e.g. [38,39]), Ca-ATPase and Mg-ATPase, respectively. We also used μCT-scans to analyse shell density and internal structures.

2. Material and methods

(a) Sample collection

Dead coral reef rubble samples containing *A. lessonii* were collected by SCUBA divers from Heron Island (23°26′51.7″ S, 151°54′45″ E) at depths ranging from 6 to 10 m in April 2013, using long-established sampling procedures (e.g. [40]). Pieces of coral rubble were brought to the surface and scrubbed using a toothbrush. Residual sediments were kept in plastic containers until transport to the Australian Institute of Marine Sciences (AIMS), Townsville, Australia. Upon arrival at the laboratory, the sediment samples were transferred to glass Petri dishes and placed undisturbed for 24 h in a flow-through aquarium system. Afterwards, adult *A. lessonii* individuals were extracted and separated for the experiment. Adult specimens of *M. vertebralis* were removed from the substrate on the reef flat at Green Island (16°45′37.5″ S, 145°58′18.5″ E) from depths between 0.6 and 0.9 m in April 2013. They were separated and held undisturbed in plastic jars within a flow-through aquarium system prior to the start of the experiment. Adult individuals were used in this study as they were abundant at collection sites.

(b) Experimental set-up

We studied the effect of decreased pH/increased pCO_2 on foraminiferal calcification in a flow-through system (400 ml min^{-1}) using natural seawater over a period of 30 days in a climate-controlled aquaria room (25 ± 1°C). Incoming seawater was filtered through a series of three filters (5 μm, 1 μm, 1 μm) into four storage tanks to remove very fine sediments. Nitrate and

phosphate levels measured in the water were 0.97 ± 0.1 and 0.2 ± 0.07 µmol l^{-1}, respectively. Salinity in the tanks was approximately 35–36, similar to values at sampling sites. As treatments, we chose four pH_{NBS} levels of 8.1, 7.9, 7.7 and 7.6, representing a range of approximately 430 to 2000 µatm pCO_2 (table 1), as this is the pH range predicted by the end of the century and thus considered ecologically relevant [2]. Four replicate glass aquaria per treatment were set up and water was pumped into each treatment aquarium via submersible pumps from four storage tanks, where the desired pCO_2 level was regulated using a CO_2 injection system (AquaMedic, Germany). The system consisted of computer-controlled solenoid valves regulated via a feedback control, set to open and close when the pH rose above or below, respectively, the target pH in the storage tanks. Monitoring of the pH at each storage tank and aquaria was performed using pH electrodes (± 0.01 pH unit) calibrated with standard US National Bureau of Standards (NBS) buffers. In addition, pH measurements were taken daily using a hand-held pH metre. Water temperature in each storage tank was recorded throughout the experiment using HOBO temperature loggers. Light was supplied using 10 000 K LED lights (55 W) and light levels were determined by a light-meter LI-1400 (LI-COR, NE, USA). Foraminifera were kept under a 12 h light/dark cycle. Each aquarium housed two 70 mm glass Petri dishes containing 40 specimens of *A. lessonii* each and two 10 ml glass vials (approx. 1 cm aperture) each containing 20 specimens of *M. vertebralis* for the biomarkers analyses. Additionally, one Petri dish containing two specimens of *A. lessonii* and one vial containing two specimens of *M. vertebralis* were deployed to analyse growth rates. Petri dishes containing *A. lessonii* individuals were covered with a 250 µm mesh, whereas *M. vertebralis* vials were covered with a 500 µm mesh to prevent individuals from crawling out. Light levels were further adjusted according to each species' requirement. Therefore, *A. lessonii* samples were wrapped with double-layer shade cloth in order to achieve a low light regime (25 µmol photons m^{-2} s^{-1}), whereas *M. vertebralis* were maintained under a slightly higher light regime (40 µmol photons m^{-2} s^{-1}). Irradiance levels chosen were based on previous experiments [23,41]. Moreover, these levels are similar to the ones found for these species at their natural microhabitat [42,43]. DIC and total alkalinity (A_T) concentrations were analysed from seawater samples collected weekly throughout the experiment from each treatment tank. Samples were analysed using the VINDTA 3C system at 24°C and salinity 33 (Marianda, Germany; precision of ± 1 µmol kg^{-1}–SW for DIC and A_T). DIC and pH values were used to calculate pCO_2, DIC and concentrations of CO_3^{2-}, as well as calcite saturation state values (Ω_{Ca}) using the software CO2SYS [44]. Carbonate parameters were calculated using K1 and K2 equilibrium constants as described by Mehrbach *et al.* [45] and modified by Dickson & Millero [46] (table 1; electronic supplementary material, table S1).

(c) Determination of surface area and buoyant weight

Surface area was determined by digital photographs taken of the cross-sectional shell surface area (e.g. [23]). Initial *A. lessonii* individuals' size varied from approximately 0.21 to 0.25 mm^2, whereas *M. vertebralis* ranged from approximately 8.06 to 16.55 mm^2. Photographs were taken from each sample using two normal appearing individuals with uniform colour displaying pseudopodial activity (indicative of health) and randomly assigned at the start of the experiment; the same individuals were identified and assessed at the end of the experiment. Photographs were analysed using ImageJ v. 1.48 [47] to automatically trace the outline and surface area of the specimens and compare their surface area gain (derived from pixel area gain) between the initial and final measurements. Buoyant weight differences were also quantified for the same individuals at the start and end of each experiment. At the end of the experiment, specimens were soaked in 10% solution of commercial bleach (42 g NaClO l^{-1}) in

Table 1. Seawater and carbonate system parameters for the 30 day experiment (mean ± s.e.; $n = 16$). (Calculated parameters were adjusted from DIC and pH values using CO2SYS software.)

measured parameters				calculated parameters			
treatment	T (°C)	A_T (µmol kg^{-1} – SW)	DIC (µmol kg^{-1} – SW)	pH (NBS)	DIC (µmol kg^{-1} – SW)	pCO_2 (µatm)	CO_3^{2-} (µmol kg^{-1} – SW)	Ω_{Ca}
pH 8.1 (ambient)	24.2 ± 0.2	2267 ± 3	1978 ± 12	8.15 ± 0.02	1974 ± 12	430 ± 23	195 ± 8	4.7 ± 0.2
pH 7.9	24.1 ± 0.2	2272 ± 4	2058 ± 10	7.89 ± 0.01	2058 ± 10	855 ± 30	113 ± 3	2.7 ± 0.1
pH 7.7	24.2 ± 0.1	2273 ± 4	2098 ± 13	7.76 ± 0.01	2097 ± 14	1168 ± 36	87 ± 3	2.1 ± 0.1
pH 7.6	24.2 ± 0.1	2275 ± 5	2130 ± 20	7.63 ± 0.02	2130 ± 19	2015 ± 20	67 ± 3	1.6 ± 0.1

seawater overnight to remove the organic matter. Percentage of total shell weight derived from organic matter was calculated for each specimen, and values subtracted from individual weight at the start of the experiment. On average, organic matter accounted for 2–3% of the total shell weight. Specimens were immersed into a vial containing 1 ml of seawater at 25°C with known density and the displaced volume weighed using a fine scale balance with a precision of 0.01 mg (Shimadzu AUW120D, Australia). Buoyant weight (BW) was calculated using the following equations:

$$\text{density} = \frac{(\text{weight in air} \times \text{density (water)})}{(\text{weight in air} - \text{weight in water})},$$

$$\text{volume} = \frac{\text{mass displaced in water}}{\text{density (water)}}$$

and

$$\text{BW} = \text{volume (LBF)} \times [\text{density (LBF)} - \text{density (water)}].$$

Growth (% growth d^{-1}) was determined following Ter Kuile & Erez [48] for both surface area and BW parameters.

(d) Micro-computer tomography scanning for shell density analysis

Shell density analysis was performed on a SkyScan 1174 (Bruker microCT, Belgium), a high-resolution desktop X-ray scanner, capable of producing two-dimensional shadow images of complete internal three-dimensional structures without chemical fixation. The µCT-scan allows non-destructive study of density and internal structures of the foraminiferal shell [33]. Five specimens from each treatment were randomly selected for this analysis. Individuals were cleaned using a fine brush, washed in deionized water and oven-dried at 37°C. *Amphistegina lessonii* and *M. vertebralis* individuals were scanned using 6.7 and 9.6 µm magnification, respectively, in a 180° rotation using a 0.5 mm Al filter at 50 kv and 800 µA. Subsequently, cross-section images were reconstructed using the software SkyScanNRecon and imaged using the software DataViewer (Bruker microCT). Foraminifera shell density values were calculated using water and pure aragonite as standards and processed in the software CT-Analyser (Bruker microCT).

(e) Analysis of Ca-aTPase and Mg-aTPase activities

Foraminifera were analysed at the beginning and after 15 and 30 days of the experiment. Samples containing 20 individuals were homogenized in a buffer solution containing 500 mM sucrose, 150 mM KCl, 20 mM Tris-Base, 1 mM DL-dithiothreitol and 0.1 mM phenylmethylsulfonyl, with pH adjusted to 7.6. Homogenates were then centrifuged at 10 000*g* for 20 min at 4°C. The resulting supernatant was adjusted to a concentration of 0.1 mg of protein ml^{-1}, which was determined using the Quant-iT Protein Assay (Life Technologies, Victoria, Australia). Filtered seawater was used as a control. Ca-ATPase was measured according to a modified protocol originally developed by Chan *et al*. [49], using a working buffer containing 80 mM NaCl, 20 mM of Tris-Base, 15 mM KCl and 15 mM $CaCl_2$. Mg-ATPase was measured using a similar working buffer; however, instead of $CaCl_2$, 15 mM $MgCl_2$ were added following Busacker & Chavi [50]. Ca-ATPase buffer was adjusted to pH 7.5 while the buffer for Mg-ATPase detection was adjusted to pH 8.1. Afterwards, samples were incubated with 250 µl of working buffer containing 1 mM of ouabain and placed into a water bath at 30°C for 30 min. The reaction was started by the addition of 3 mM ATP and stopped by placing the samples in ice for 10 min. Samples were analysed following the method of Fiske & Subbarow [51]. Using this method, the inorganic phosphate (P_i) released from the ATP consumption during calcium and magnesium pumping is measured. P_i concentration in the reaction mixture was quantified by spectrophotometry (620 ηm) using an ELx 808 absorbance microplate reader (BioTek, VT, USA). P_i concentration was determined using a phosphate kit (BioVision, CA, USA) and calculated using a calibration curve constructed with P_i standards (10 mM). Ca/Mg-ATPase activities were calculated as µmoles P_i mg $protein^{-1}$ h^{-1}.

(f) Data analyses

Mixed-model analysis of variance (ANOVA), using *aquarium* as a nested factor was performed to test whether decreasing pH levels had an effect on growth rates after 30 days. If indicated, ANOVA were followed by post hoc Tukey's (HSD) test. One-way ANOVA was carried out to compare differences in densities among treatments. Linear regression was performed to investigate the relationship between buoyant weight and surface area for each experimental condition and species. The relationship between size and weight is defined by a power function, and so it is expected to be uniform between treatments. Data were log transformed and the slope of the linearized function, which defines the relationship between buoyant weight and surface area from each curve (treatment group), was compared using Student's *t*-test. Two-way ANOVA followed by the HSD test, if indicated, was used to test the effect of pH through time on the enzymatic activity of each species, using pH levels and time as fixed factors. Results are expressed as mean ± 1 s.e.m. All data were checked for homogeneity of variance as well as normality prior to ANOVA using Levene's and Shapiro–Wilk's tests, respectively. Because growth rates are expressed as percentages, data were arcsine-square-root transformed preceding ANOVA. In all cases, significance level adopted was 95% ($\alpha = 0.05$).

3. Results

(a) Growth in different pH levels

Growth rate expressed as surface area was not significantly affected by low pH conditions for both *A. lessonii* and *M. vertebralis* (figure 1; electronic supplementary material, tables S2 and S12). However, pH significantly affected buoyant weight growth rates in *A. lessonii* (figure 1*a*). A steady reduction of buoyant weight growth rates was observed for *A. lessonii* with the gradual decrease of pH in the water; however, significant differences were only observed at pH levels of 7.7 and 7.6, where a reduction of approximately 50% was detected (figure 1*a*; electronic supplementary material, table S3). No significant difference in surface area and buoyant weight was observed for *M. vertebralis* among the pH treatments (figure 1*b*; electronic supplementary material, table S4). The relationship between surface area and BW varied in *A. lessonii* with exposure to different pH conditions, as specimens of a given surface area cultured at pH below 7.9 are less dense when compared to those grown at ambient conditions (figure 2). Specimens grown under pH 7.7 and 7.6 also grew less (measured as increase in surface area) than those exposed to ambient pH conditions (figure 1*a*; electronic supplementary material, figure S1*a*). In *M. vertebralis*, a statistical comparison of the slopes of the surface area to buoyant weight relationship showed that the slope at pH 7.9 was significantly different from those at all other treatments (Student's *t*-test; ambient: $p < 0.01$; pH 7.9: $p < 0.01$; pH 7.6: $p < 0.01$; electronic supplementary material, table S5). However, no significant difference in size and growth rates was observed.

(b) Micro-computer tomography scan images and shell density analysis

µCT scan images showed that shell density of *A. lessonii* individuals cultured at pH 7.6 was approximately 20% lower when

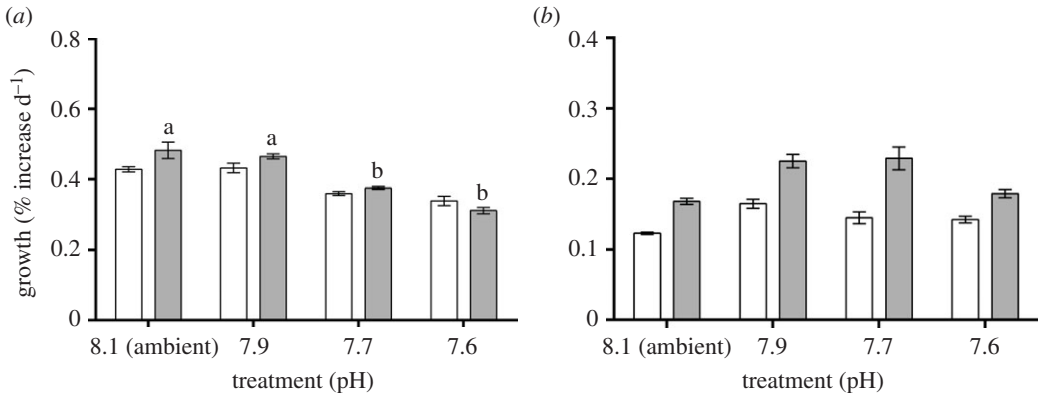

Figure 1. Growth rates expressed as surface area (white bars) and buoyant weight (grey bars) of (*a*) *A. lessonii* and (*b*) *M. vertebralis* in the 30 day experiment. Data are expressed as mean ± s.e. ($n = 12$). Different letters indicate statistically significant differences (Tukey's HSD test; $p < 0.05$) in mean values among experimental groups of individuals. Upper and lower bars indicate standard error of the mean.

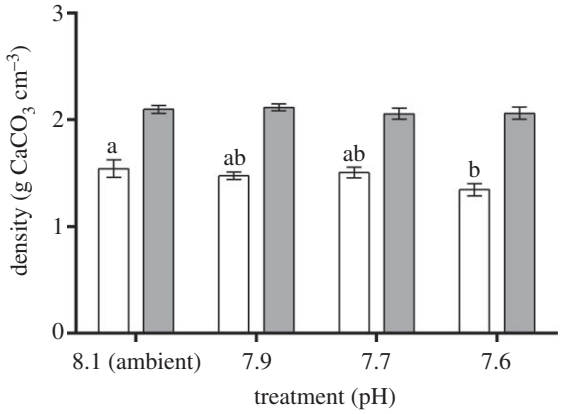

Figure 2. Density of *A. lessonii* (white bars) and *M. vertebralis* (grey bars) individuals exposed to different pH conditions. Data are expressed as mean ± s.e. ($n = 5$). Different letters (a, b) indicate statistically significant differences (Tukey's HSD test; $p < 0.05$) in mean values among experimental groups of individuals. Upper and lower bars indicate standard error of the mean.

compared with individuals exposed to ambient pH conditions after 30 days (figures 2 and 3*a*; electronic supplementary material, table S12). Density values dropped from 1.54 ± 0.03 to 1.34 ± 0.02 g cm^{-3} (ANOVA; $F_{3,19} = 10.32$; $p < 0.01$; electronic supplementary material, table S6). Conversely, *M. vertebralis* images showed no difference regarding internal shell density among treatments (ANOVA; $F_{3,19} = 2.25$; $p = 0.12$; figures 2 and 3*b*; electronic supplementary material, table S7).

(c) Effects on the calcification enzymes

In general, a decrease in pH levels resulted in a significant rise of enzyme activity in *A. lessonii* (ANOVA; $F_{3,84} = 37.58$; $p < 0.01$; figure 4*a*,*b*). The lowest pH treatment had significantly increased enzyme activity compared with ambient pH conditions (electronic supplementary material, tables S8 and S9), and Ca-ATPase and Mg-ATPase activities were raised twofold after 30 days of exposure (figure 4*a*,*b*). However, no significant effect was observed for Ca-ATPase activity in *M. vertebralis* among treatments (figure 4*c*), and a significant inhibition of approximately 30% of Mg-ATPase activity was observed in those individuals exposed to pH levels below ambient conditions only at the end of the 30 day period (ANOVA; $F_{6,84} = 14.50$; $p < 0.01$; electronic supplementary material, tables S8 and S10). Activity declined from 1.24 ± 0.06 to 0.89 ± 0.02 µmoles P_i mg protein^{-1} h^{-1}, in the ambient and lowest pH levels, respectively (ANOVA; $F_{3,84} = 11.56$; $p < 0.01$; figure 4*d*; electronic supplementary material, tables S8 and S12).

4. Discussion

The LBF species *A. lessonii* and *M. vertebralis* contrast in the type of calcite they precipitate, calcification mechanisms and the symbionts that they host. Our experiment indicates substantial differences in their morphological and biochemical responses to decreasing pH/increasing pCO_2 levels. We suggest that differences in calcification mechanisms and shell morphology (i.e. perforate versus imperforate shells) rather than different endosymbionts have an important influence on how these organisms respond to increasing OA.

(a) Diatom-bearer, low-Mg calcite *Amphistegina lessonii*

Growth rates in *A. lessonii* specimens exposed to seawater with reduced pH were affected after 30 days of exposure. A similar pattern was observed in specimens of *Ammonia tepida* that developed lighter shells incubated under elevated pCO_2 levels than those grown under ambient conditions [13]. *Ammonia tepida* is a symbiont-free species, and even though both species are considered low-Mg calcite, perforate species, the amount of Mg^{2+} present in *A. lessonii* is approximately 100× higher than *Amm. tepida* [13,37]. By contrast, Hikami *et al.* [52] observed enhanced growth (as shell weight) of the diatom-bearing foraminifera *Calcarina gaudichaudii* and attributed it to the presence of symbionts, which can benefit from high-CO_2 conditions. Although *A. lessonii* and *C. gaudichaudii* harbour the same symbiont species, they differ in concentration of Mg^{2+} ions in their calcite [37]. Moreover, it is possible that *A. lessonii* and *C. gaudichaudii* are adapted to different environmental conditions of pH, as *C. gaudichaudii* is mainly found on the reef flat [34] where pH levels are more variable than on the reef slope (e.g. [53]). Therefore, the energy required by *A. lessonii* for calcification and to cope with more acidic conditions is potentially greater than that required by *C. gaudichaudii*.

Growth measured as surface area was not affected by decreasing pH levels, but buoyant weight in *A. lessonii* declined after 30 days. µCT scanning analysis showed that the density of the inner-shell and older chambers of

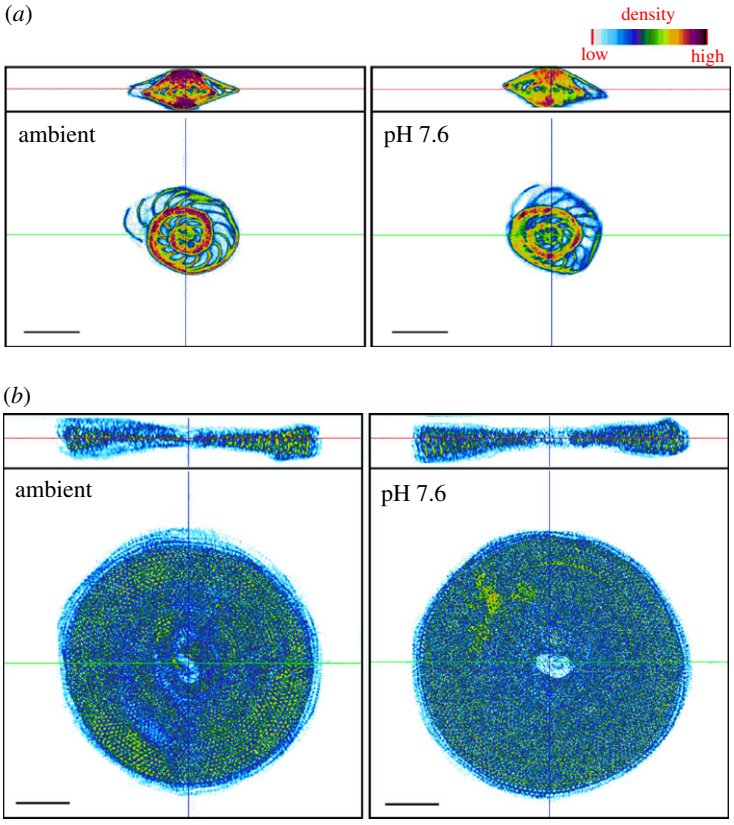

Figure 3. Comparison between X-ray images from (*a*) *A. lessonii* and (*b*) *M. vertebralis* exposed to ambient and pH 7.6 conditions after 30 days. Colour scale represents relative density values. Scale bar, 1 mm. (Online version in colour.)

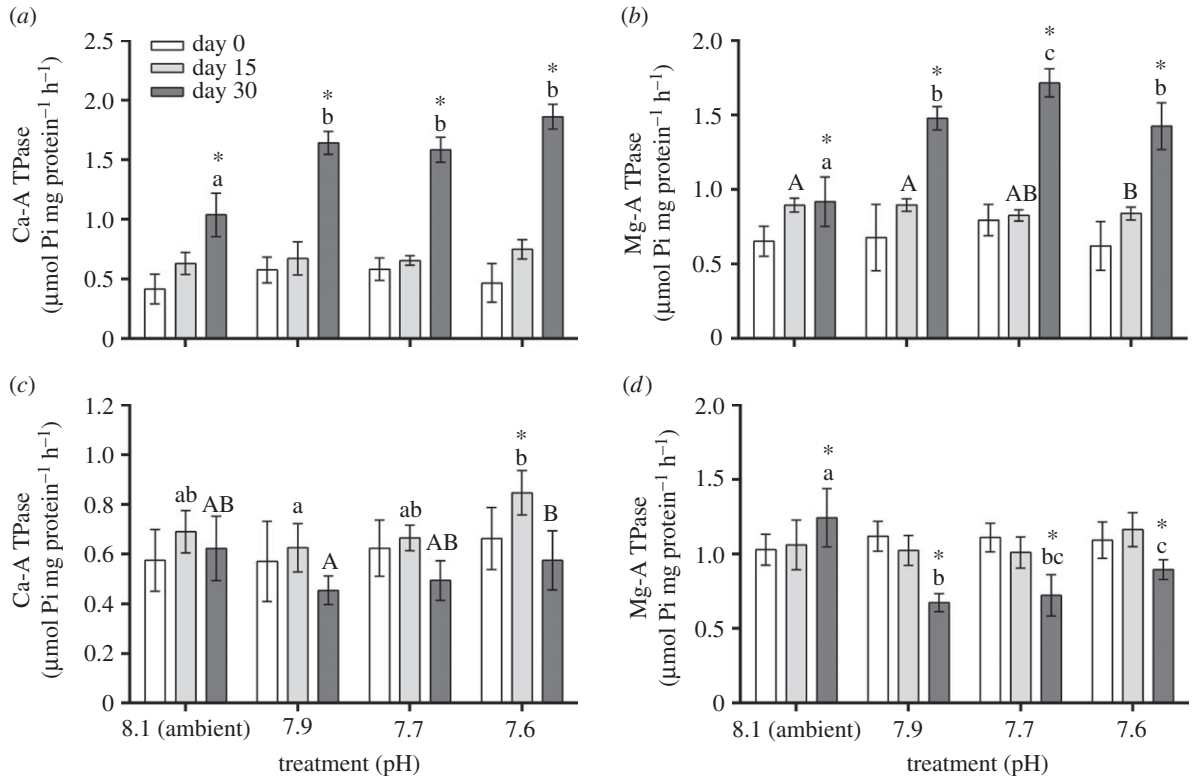

Figure 4. (*a*) Ca-ATPase and (*b*) Mg-ATPase activity in holobionts of *A. lessonii*; and (*c*) Ca-ATPase and (*d*) Mg-ATPase enzymatic activity in *M. vertebralis* exposed to different pH treatments. Data are expressed as mean $\pm$ s.e. ($n = 8$). Different small and capital letters indicate statistically significant differences (Tukey's HSD test; $p < 0.05$) in mean values among experimental groups of individuals. Asterisks (*) indicate significantly different mean values among times within each experimental condition. Upper and lower bars indicate standard error of the mean.

individuals exposed to pH 7.6/2000 µatm CO_2 was reduced relative to those in control aquaria exposed to ambient conditions (figure 3*a*), even though Ω_{Ca} was above 1 (table 1). It is likely that the decrease in shell density resulted in lower buoyant weight in *A. lessonii* exposed to pH 7.6. Shell dissolution at $\Omega_{Ca} > 1$ was also observed in live specimens

of congeneric *Amphistegina gibbosa* individuals exposed to 1000 and 2000 µatm CO_2 [25], suggesting that even when alive these foraminifera cannot avoid partial dissolution of their shell under reduced pH. We suggest that the dissolution suffered passively by *A. lessonii* exposed to low pH/high CO_2 levels is likely to be the result of the incapacity of foraminifera to repair their shells while maintaining cellular homeostasis, as maintenance of shell integrity may require continuous energy investment (e.g. [54]).

In *A. lessonii*, both enzymes Ca- and Mg-ATPases are highly activated, most likely removing Ca^{2+} and Mg^{2+} ions that are released as a result of dissolution. Glas *et al.* [17] showed experimentally that no significant changes occurred in the variation of Ca^{2+} concentration in the foraminifera's microenvironment. By contrast, we detected changes in Ca-ATPase activity with shifts in pH levels (figure 4*a*). Because Ca^{2+} is a very important cofactor for the functions of many enzymes and can be cytotoxic in high concentrations [55], foraminifera must have an internal auto-regulatory system, in which rapid changes in Ca-ATPase activity (this study) can be compensated via other Ca^{2+} channels [56]. Alternatively, as the concentration of CO_3^{2-} decreases with declining pH levels, Ca-ATPase is upregulated in order to maintain Ω_{Ca} in the calcification media [57]. The observed enhanced activity at ambient levels is likely to be a result of a natural decline in Ω_{Ca} values towards the end of the experiment (electronic supplementary material, table S1). A similar pattern was also observed for Mg-ATPase, which in this case would remove Mg^{2+} ions from the intracellular media, as Mg^{2+} ions prevent calcite precipitation when found in high concentrations [58].

(b) Dinoflagellate-bearer, high-Mg calcite *Marginopora vertebralis*

In contrast to *A. lessonii*, our results showed that growth rates of *M. vertebralis* were not affected by changes in pH levels. Nonetheless, is important to note that even with an unequal mean size distribution at the outset of the experiment, we did not observe significant differences in growth rates between treatments. Similar results were also found by Vogel & Uthicke [23], who also observed either no effect or enhanced growth in *M. vertebralis* after 45 days exposure to as high as 1925 ppm CO_2. Conversely, a decline in shell weight of newly asexually produced specimens of *Amphisorus hemiprichii* was detected by Hikami *et al.* [52] after four weeks exposed to low pH/high pCO_2 conditions. Both species live on and are adapted to the shallow areas of the reef [34]. In this case, differences in responses observed might be explained by the fact that individuals from early stages and juveniles can be more sensitive and susceptible to changes in environmental conditions (e.g. [59]). Nonetheless, although we detected no significant direct effect on growth rates of *M. vertebralis* and Ca-ATPase activity, increasing pCO_2 levels resulted in a significant decline of holobiont Mg-ATPase activity (figure 4*c*,*d*).

Ca-ATPase activity of *M. vertebralis* exposed to low pH/high CO_2 levels increased in the first 15 days for all treatments, than dropped by the end of the experiment. However, significant differences were only observed at pH 7.6 (figure 4*c*). In this case, it is likely that the reduction in Ca-ATPase activity is a natural consequence rather than an effect of changes in pH levels, as growth rates of *M. vertebralis* were not affected by these changes (figure 1*b*).

On the other hand, Mg-ATPase activity declined with decreasing in pH levels (figure 4*d*). Ter Kuile *et al.* [22] found that the high-Mg calcite foraminifera *Amphisorus hemprichii* depends less on ATP than low-Mg species such as *A. lessonii*. It is likely that less energy is needed by high-Mg species when subjected to stressful conditions, which might affect the precipitation of calcite. Consequently, the inhibition or reduced activity of Mg-ATPase, which plays a role in removing Mg^{2+} ions (e.g. [38]), could be a strategy to cope with different pH/pCO_2 conditions. Alternatively, in order to sustain calcification and Ca-ATPase activity constants, less energy could be available for maintenance of Mg-ATPase activity. Reymond *et al.* [26] suggested that precipitation of the high-Mg calcite in congener *Marginopora rossi* would be impaired at pH 7.6 probably owing to changes in HCO_3^- and H^+ concentration in the surrounding water, which alter the intracellular chemistry needed for calcification. However, our experiment indicated that *M. vertebralis* continues to add chambers, increasing in both size and weight regardless of changes in seawater chemistry conditions. *Marginopora vertebralis* is mainly found in shallow areas around reef flats, where daily CO_2 and pH levels are much more variable than at depth (e.g. [53]), and are thus likely to be more adapted and less sensitive to changes in carbonate chemistry than *M. rossi*, which dwell in deeper, more stable environments (e.g. [26]).

(c) The role of the symbionts

Amphistegina lessonii and *M. vertebralis* not only differ in skeletal chemistry but also symbiont group. Both diatoms and dinoflagellate endosymbionts use CO_2 primarily as an inorganic C source, but they also use HCO_3^{2-} for photosynthesis [22]. Previous experiments with *Amphistegina radiata* and *M. vertebralis* showed that photosynthesis was either not affected or increased with greater levels of CO_2 [11,23], and rates of photosynthesis in both diatom and dinoflagellate symbionts can be enhanced by acidic conditions as CO_2 and HCO_3^- increase in the water [23]. Because foraminifera rely on CO_3^{2-} [60] for calcification this might explain why calcification is often affected by OA, while photosynthetic rates remain unchanged. Incorporation of DIC through photosynthesis and calcification in both low- and high-Mg calcite foraminifera are not linked obligatorily, but instead may compete for the same DIC source [22].

Even though both perforate, low-Mg calcite and imperforate, high-Mg calcite foraminifera species have an internal inorganic C pool which serves mainly for calcification but also photosynthesis [16,57], they differ in calcification pathways [16]. Thus, although symbionts play an important role in providing energy to their respective hosts [61], we suggest that the differences in responses observed between *A. lessonii* and *M. vertebralis* are owing more to differences in calcification mechanisms rather than symbiont type.

(d) The possible role of Ca- and Mg-ATPase in calcification

The presence of transmembrane transporters that regulates intracellular Ca^{2+} and Mg^{2+} balance in foraminifera was suggested by Erez [19], Nehrke *et al.* [56] and Bentov & Erez [62], but enzymes that regulate ions balance in foraminifera have not yet been identified. In both low-Mg, perforate species (such as *A. lessonii*) and high-Mg, imperforate *M. vertebralis*,

Ca-ATPase appears to play an important role in actively regulating intracellular Ca^{2+} balance. The increase in Ca-ATPase in *A. lessonii* suggests that when dissolution occurs (figures 3*a* and 4*a*) resulting in the release of Ca^{2+} ions into the cell, this enzyme is upregulated. However, as no significant effect on growth and calcification of *M. vertebralis* was detected, Ca-ATPase activity was not affected. Moreover, baseline Ca-ATPase activity is equal in both species, at approximately 0.6 µmoles P_i mg protein^{-1} h^{-1} (figure 4*a*,*c*).

Mg-ATPase activity seems to be more sensitive to changes in pH/pCO_2 conditions than Ca-ATPase, as the Mg-ATPase activity was affected in both species studied here. Although still poorly known in foraminifera, our results suggest that Mg-ATPase is likely to play a role in regulating the concentration of Mg^{2+} inside the calcification site so high- or low-Mg calcite can be precipitated accordingly [16]. *Marginopora vertebralis* precipitates calcite with high-Mg^{2+} content (more than 20 moles% $MgCO_3$), and as such these individuals do not need to eliminate as much Mg^{2+} as low-Mg-calcite foraminifera (less than 6 moles% $MgCO_3$; [54]). Consequently, there is an energetic advantage to allow the Mg^{2+} to remain in the calcifying fluid. Interestingly, baseline Mg-ATPase activity of *A. lessonii* is approximately 50% lower than in *M. vertebralis* (figure 4*b*,*d*). As suggested by Nehrke *et al*. [56], the discrimination of a typical Ca^{2+} channel against Mg^{2+} is very strong, and it is possible that the pseudopodial network in perforate species is temporarily or permanently leaky, meaning that only a small amount of Mg^{2+} would ultimately enter the calcification space.

5. Conclusion

Our results provide insights into the role of enzymes that transport and regulate Ca^{2+} and Mg^{2+} ions in starting the precipitation of calcite and how they are affected by changes in pH levels. Even though the biochemical apparatus of both species are affected by the rise in CO_2 concentrations, no mortality was observed throughout the experiment. Nevertheless, because pH and carbonate system parameters covary, it is difficult to identify which of the parameters are causing the effects observed. The differences in biochemical/morphological responses between *A. lessonii* and *M. vertebralis*, involving the calcification process, demonstrate their individual ability to function under reduced Ω_{Ca}. The physiological mechanisms involved in calcification, although not fully understood, indicate that LBF are still able to calcify under predicted OA conditions by regulating enzymatic activity and that responses are species-specific.

Amphistegina lessonii, which hosts diatoms and deposits low-Mg calcite, is more sensitive to changes in pH conditions than *M. vertebralis*, with different symbiont type and skeleton composition. We suggest that one of the factors responsible for these differences in response is the calcification enzymes, which regulate biochemical functions involved in the different calcification pathways and may have ultimately allowed *M. vertebralis* to overcome its more susceptible mineralogy [63]. Other factors such as the capacity for species to adapt in order to survive substantial variability should also be considered [25], as both the short-term and evolutionary scale changes under which LBF species have survived and thrive support the interpretation of adaptation to substantial ranges in carbonate saturation states [25,64]. Therefore, long-term experiments taking into consideration the local environmental variations in pH [25], and the impacts of OA over multiple generations are crucial to understand their ability to adapt to this changing world [65].

Data accessibility. Electronic supplementary material is available digitally at Dryad Digital Repository (doi:10.5061/dryad.28816).

Acknowledgements. We would like to thank Heron Island Research Station staff for support in the field and Yan Xiang Ow for her assistance in conducting the experiment at the Australian Institute of Marine Science; Stephen Boyle and Jane Wu Won for processing the water samples for nutrients and carbonate system parameters; Maria Gomez Cabrera for her assistance in processing the X-ray images and Neal Cantin for the loan of the µCT-scan standards. We are grateful to Pamela Hallock Muller and Nina Keul for their comments, which greatly improved the manuscript.

Funding statement. This research was funded by the ARC Centre of Excellence for Coral Reef Studies grant to J.M.P. and others and the Australia's National Environmental Research Program (NERP) Tropical Ecosystems Hub grants to J.M.P., S.U. and others.

References

1. Hilmi N *et al*. 2013 Towards improved socio-economic assessments of ocean acidification's impacts. *Mar. Biol.* **160**, 1773–1787. (doi:10.1007/s00227-012-2031-5)
2. Moss RH *et al*. 2010 The next generation of scenarios for climate change research and assessment. *Nature* **463**, 747–756. (doi:10.1038/nature08823)
3. Stocker TF *et al*. 2013 *Climate change 2013: the physical science basis. Contribution of Working Group I to the Fifth Assessment Report of the Intergovernmental Panel on Climate Change*. Cambridge, UK: Cambridge University Press.
4. Doney SC, Fabry VJ, Feely RA, Kleypas JA. 2009 Ocean acidification: the other CO_2 problem. *Annu. Rev. Mar. Sci.* **1**, 169–192. (doi:10.1146/annurev.marine.010908.163834)
5. Howard WR *et al*. 2012 Ocean acidification. In *A marine climate change impacts and adaptation report card for Australia 2012* (eds ES Poloczanska, AJ Hobday, AJ Richardson). See http://www.oceanclimatechange.org.au.
6. Uthicke S, Furnas M, Lønborg C. 2014 Coral reefs on the edge? Carbon chemistry on inshore reefs of the Great Barrier Reef. *PLoS ONE* **9**, e109092. (doi:10.1371/journal.pone.0109092)
7. Kroeker KJ, Kordas RL, Crim R, Hendriks IE, Ramajo L, Singh GS, Duarte CM, Gattuso J-P. 2013 Impacts of ocean acidification on marine organisms: quantifying sensitivities and interaction with warming. *Glob. Change Biol.* **19**, 1884–1896. (doi:10.1111/gcb.12179)
8. Ries JB, Cohen AL, McCorkle DC. 2009 Marine calcifiers exhibit mixed responses to CO_2-induced ocean acidification. *Geology* **37**, 1131–1134. (doi:10.1130/G30210A.1)
9. Fabricius KE *et al*. 2011 Losers and winner in coral reefs acclimatized to elevated carbon dioxide concentrations. *Nat. Clim. Change* **1**, 165–169. (doi:10.1038/nclimate1122)
10. Fujita K, Hikami M, Suzuki A, Kuroyanagi A, Sakai K, Kawahata H, Nojiri Y. 2011 Effects of ocean acidification on calcification of symbiont-bearing reef foraminifers. *Biogeosciences* **8**, 2089–2098. (doi:10.5194/bg-8-2089-2011)
11. Uthicke S, Fabricius KE. 2012 Productivity gains do not compensate for reduced calcification under near-future ocean acidification in the photosynthetic benthic foraminifer species *Marginopora vertebralis*. *Glob. Change Biol.* **18**, 2781–2791. (doi:10.1111/j.1365-2486.2012.02715.x)

12. Pandolfi JM, Connolly SR, Marshall DJ, Cohen AL. 2011 Projecting coral reef futures under global warming and ocean acidification. *Science* **333**, 418–422. (doi:10.1126/science.1204794)
13. Dissard D, Nehrke G, Reichart GJ, Bijma J. 2010 Impact of seawater pCO_2 on calcification and Mg/Ca and Sr/Ca ratios in benthic foraminifera calcite results from culturing experiments with *Ammonia tepida*. *Biogeosciences* **7**, 81–93. (doi:10.5194/bg-7-81-2010)
14. Langer MR, Silk MT, Lipps JH. 1997 Global ocean carbonate and carbon dioxide production: the role of reef foraminifera. *J. Foramin. Res.* **27**, 271–277. (doi:10.2113/gsjfr.27.4.271)
15. Tambutté S, Holcomb M, Ferrier-Pagès C, Reynaud S, Tambutté E, Zoccola D, Allemand D. 2011 Coral biomineralization: from the gene to the environment. *J. Exp. Mar. Biol. Ecol.* **408**, 58–78. (doi:10.1016/j.jembe.2011.07.026)
16. Nooijer LJ, Toyofuku T, Kitazato H. 2009 Foraminifera promote calcification by elevating their intracellular pH. *Proc. Natl Acad. Sci. USA* **106**, 15 374–15 378. (doi:10.1073/pnas.0904306106)
17. Glas MS, Fabricius KE, de Beer D, Uthicke S. 2012 The O_2, pH and Ca^{2+} microenvironment of benthic foraminifera in a high CO_2 world. *PLoS ONE* **7**, e50010. (doi:10.1371/journal.pone.0050010)
18. Hallock P. 1981 Production of carbonate sediments by selected large benthic foraminifera on two Pacific coral reefs. *J. Sediment. Petrol.* **51**, 467–474. (doi:10.1306/212F7CB1-2B24-11D7-86480001 02C1865D)
19. Erez J. 2003 The source of ions for biomineralization in foraminifera and their implications for paleoceanographic proxies. *Rev. Mineral. Geochem.* **54**, 115–149. (doi:10.2113/0540115)
20. Hallock P, Williams DE, Fisher EM, Toler SK. 2006 Bleaching in foraminifera with algal symbionts: implications for reef monitoring and risk assessment. *Anu. Inst. Geociênc.* **29**, 108–128.
21. Bentov S, Brownlee C, Erez J. 2009 The role of seawater endocytosis in the biomineralization process in calcareous foraminifera. *Proc. Natl Acad. Sci. USA* **106**, 21 500–21 504. (doi:10.1073/pnas.0906636106)
22. Ter Kuile B, Erez J, Padan E. 1989 Mechanisms for the uptake of inorganic carbon by two species of symbiont-bearing foraminifera. *Mar. Biol.* **103**, 241–251. (doi:10.1007/BF00543354)
23. Vogel N, Uthicke S. 2012 Calcification and photobiology in symbiont-bearing benthic foraminifera and responses to a high CO_2 environment. *J. Exp. Mar. Biol. Ecol.* **424–425**, 15–24. (doi:10.1016/j.jembe.2012.05.008)
24. Kuroyanagi A, Kawahata H, Suzuki A, Fujita K, Irie T. 2009 Impacts of ocean acidification on large benthic foraminifers: results from laboratory experiments. *Mar. Micropaleontol.* **73**, 190–195. (doi:10.1016/j.marmicro.2009.09.003)
25. McIntyre-Wressnig A, Bernhard JM, McCorkle DC, Hallock P. 2013 Non-lethal effects of ocean acidification on the symbiont-bearing benthic foraminifer *Amphistegina gibbosa*. *Mar. Ecol. Prog. Ser.* **472**, 45–60. (doi:10.3354/meps09918)
26. Reymond CE, Lloyd A, Kline DI, Dove SG, Pandolfi JM. 2013 Decline in growth of foraminifer *Marginopora rossi* under eutrophication and ocean acidification scenarios. *Glob. Change Biol.* **19**, 291–302. (doi:10.1111/gcb.12035)
27. Schmidt C, Kucera M, Uthicke S. 2014 Combined effects of warming and ocean acidification on coral reef foraminifera *Marginopora vertebralis* and *Heterostegina depressa*. *Coral Reefs* **33**, 805–818. (doi:10.1007/s00338-014-1151-4)
28. Sinutok S, Hill R, Doblin MA, Wuhrer R, Ralpha PJ. 2011 Warmer more acidic conditions cause decreased productivity and calcification in subtropical coral reef sediment-dwelling calcifiers. *Limnol. Oceanogr.* **56**, 1200–1212. (doi:10.4319/lo.2011.56.4.1200)
29. Doo SS, Fujita K, Byrne M, Uthicke S. 2014 The fate of calcifying tropical symbiont-bearing large benthic foraminifera: living sands in a changing ocean. *Biol. Bull.* **226**, 169–186.
30. Prazeres MF, Martins SE, Bianchini A. 2012 Assessment of water quality in coastal waters of Fernando de Noronha, Brazil: biomarkers analyses in *Amphistegina lessonii*. *J. Foramin. Res.* **42**, 56–65. (doi:10.2113/gsjfr.42.1.56)
31. Downs CA, Fauth JE, Robinson CE, Curry R, Lanzendorf B, Halas JC, Halas J, Woodley CM. 2005 Cellular diagnostics and coral health: declining coral health in the Florida Keys. *Mar. Pollut. Bull.* **51**, 558–569. (doi:10.1016/j.marpolbul.2005.04.017)
32. Görög A, Szinger B, Tóth E, Viszkok J. 2012 Methodology of the micro-computer tomograhy on foraminifera. *Palaeontol. Electron.* **15**, 3T.
33. Briguglio A, Hohenegger J, Less G. 2013 Paleobiological applications of three-dimensional bimetry on large benthic foraminifera: a route of new discoveries. *J. Foramin. Res.* **43**, 72–87. (doi:10.2113/gsjfr.43.1.72)
34. Hohenegger J, Yordanova E, Nakano Y, Tatzreiter F. 1999 Habitats of larger foraminifera on the upper reef slope of Sesoko Island, Okinawa, Japan. *Mar. Micropaleontol.* **36**, 109–168. (doi:10.1016/S0377-8398(98)00030-9)
35. Hohenegger J. 1994 Distribution of living larger foraminifera NW of Sesoko-Jima, Okinawa, Japan. *PSZNI Mar. Ecol.* **15**, 291–334. (doi:10.1111/j.1439-0485.1994.tb00059.x)
36. Baccaert J. 1976 Scientific report of the Belgium expedition to the Australian Great Barrier Reef, 1967. Foraminifera: Soritidae of the Lizard Island reef complex, a preliminary report. *Ann. Soc. Géol. Belgique* **99**, 237–262.
37. Raja R, Saraswati PK, Rogers K, Iwao K. 2005 Magnesium and strontium compositions of recent symbiont-bearing benthic foraminifera. *Mar. Micropaleontol.* **58**, 31–44. (doi:10.1016/j.marmicro.2005.08.001)
38. Romani AMP, Maguire ME. 2002 Hormonal regulation of Mg^{2+} transport and homeostasis in eukaryotic cells. *Biometals* **15**, 271–283. (doi:10.1023/A:1016082900838)
39. Al-Horani FA, Al-Moghrabi SM, de Beer D. 2003 The mechanism of calcification and its relation to photosynthesis and respiration in the scleractinian coral *Galaxea fascicularis*. *Mar. Biol.* **142**, 419–426. (doi:10.1007/s00227-002-0981-8)
40. Hallock P, Forward LB, Hansen HJ. 1986 Influence of environment on the test shape of *Amphistegina*. *J. Foramin. Res.* **16**, 224–231. (doi:10.2113/gsjfr.16.3.224)
41. Walker RA, Hallock P, Torres JJ, Vargo GA. 2011 Photosynthesis and respiration in five species of benthic foraminifera that host algal endosymbionts. *J. Foramin. Res.* **41**, 314–325. (doi:10.2113/gsjfr.41.4.314)
42. Fujita K. 2004 A field colonization experiment on small-scale distribution of algal symbiont-bearing larger foraminifera on reef rubble. *J. Foramin. Res.* **34**, 169–179. (doi:10.2113/34.3.169)
43. Nobes K, Uthicke S, Henderson R. 2008 Is light the limiting factor for the distribution of benthic symbiont bearing foraminifera on the Great Barrier Reef? *J. Exp. Mar. Biol. Ecol.* **363**, 48–57. (doi:10.1016/j.jembe.2008.06.015)
44. Pierrot D, Lewis ED, Wallace DW. 2006 *MS Excel Program Developed for CO_2 System Calculations*. ORNL/CDIAC-105a. Carbon Dioxide Information Analysis Center, Oak Ridge National Laboratory, U.S. Department of Energy, Oak Ridge, TN, USA. See http://dx.doi.org/10.3334/cdiac/otg.co2sys_xls_cdiac105a.
45. Mehrbach C, Culberson CH, Hawley JE, Pytkowicz RM. 1973 Measurement of the apparent dissociation constants of carbonic acid in seawater at atmospheric pressure. *Limnol. Oceanogr.* **18**, 897–907. (doi:10.4319/lo.1973.18.6.0897)
46. Dickson AG, Millero FJ. 1987 A comparison of the equilibrium constants for the dissociation of carbonic acid in seawater media. *Deep-Sea Res.* **34**, 1733–1743. (doi:10.1016/0198-0149(87)90021-5)
47. Rasband WS. 1997 *ImageJ*. Bethesda, MD: U. S. National Institutes of Health. See http://imagej.nih.gov/ij/.
48. Ter Kuile B, Erez J. 1984 *In situ* growth rate experiments on the symbiont-bearing foraminifera *Amphistegina lobifera* and *Amphisorus hemprichii*. *J. Foramin. Res.* **14**, 262–276. (doi:10.2113/gsjfr.14.-4.262)
49. Chan K-M, Delfert D, Junger KD. 1986 A direct colorimetric assay for Ca^{2+}-stimulated ATPase activity. *Anal. Biochem.* **157**, 375–380. (doi:10.1016/0003-2697(86)90640-8)
50. Busacker GP, Chavin W. 1981 Characterization of Na^+/K^+-ATPases and Mg^{2+}-ATPase from the gill and the kidney of the goldfish (*Carassius auratus* L.). *Comp. Biochem. Physiol. B* **69**, 249–256. (doi:10.1016/0305-0491(81)90237-6)
51. Fiske CH, Subbarow Y. 1925 The colorimetric determination of phosphorus. *J. Biol. Chem.* **66**, 375–400.
52. Hikami M, Ushie H, Irie T, Fujita K, Kuroyanagi A, Sakai K, Nojiri Y, Suzuki A, Kawahata H. 2011 Contrasting calcification responses to ocean acidification between two reef foraminifers

harboring different algal symbionts. *Geophys. Res. Lett.* **38**, L19601. (doi:10.1029/2011GL048501)

53. Yates KK, Halley RB. 2006 CO_2^{-3} concentration and pCO_2 thresholds for calcification and dissolution on the Molokai reef flat, Hawaii. *Biogeosciences* **3**, 357–369. (doi:10.5194/bg-3-357-2006)
54. Melzner F, Stange P, Trubenbach K, Thomsen J, Casties I, Panknin U, Gorb SN, Gutowska MA. 2011 Food supply and seawater pCO_2 impact calcification and internal shell dissolution in the blue mussel *Mytilus edulis*. *PLoS ONE* **6**, e24223. (doi:10.1371/journal.pone.0024223)
55. Rasmussen H, Barrett P, Smallwood J, Bollag W, Isales C. 1990 Calcium ion as intracellular messenger and cellular toxin. *Environ. Health Perspect.* **84**, 17–25. (doi:10.1289/ehp.908417)
56. Nehrke G, Keul N, Langer G, de Nooijer LJ, Bijma J, Meibom A. 2013 A new model for biomineralization and trace-element signatures of foraminifera tests. *Biogeosciences* **10**, 6759–6767. (doi:10.5194/bg-10-6759-2013)
57. De Nooijer LJ, Spero HJ, Erez J, Bijma J, Reichart GJ. 2014 Biomineralization in perforate foraminifera. *Earth-Sci. Rev.* **135**, 48–58. (doi:10.1016/j.earscirev.2014.03.013)
58. Köhler-Rink S, Kühl M. 2000 Microsensor studies of photosynthesis and respiration in large symbiotic foraminifera. I. The physico-chemical microenvironment of *Marginopora vertebralis*, *Amphistegina lobifera* and *Amphisorus hemprichii*. *Mar. Biol.* **137**, 473–486. (doi:10.1007/s002270000335)
59. Alve E, Goldstein ST. 2014 The propagule method as an experimental tool in foraminiferal ecology. In *Approaches to study living foraminifera: collection, maintenance and experimentation* (eds H Kitazato, JM Bernhard), pp. 1–12. Tokyo, Japan: Springer.
60. Keul K, Langer G, de Nooijer LJ, Bijma J. 2013 Effect of ocean acidification on the benthic foraminifera *Ammonia* sp. is caused by a decrease in carbonate ion concentration. *Biogeosciences* **10**, 6185–6198. (doi:10.5194/bg-10-6185-2013)
61. Lee JJ, Sang K, Ter Kuile B, Strauss E, Lee PJ, Faber Jr WW. 1991 Nutritional and related experiments on laboratory maintenance of three species of symbiont-bearing large foraminifera. *Mar. Biol.* **109**, 417–425. (doi:10.1007/BF01313507)
62. Bentov S, Erez J. 2006 Impact of biomineralization processes on the Mg content of foraminiferal shells: a biological perspective. *Geochem. Geophy. Geosyst.* **7**, Q01P08. (doi:10.1029/2005GC001015)
63. Plummer LN, Mackenzie FT. 1974 Predicting mineral solubility from rate data: application to the dissolution of magnesian calcite. *Am. J. Sci.* **274**, 61–83. (doi:10.2475/ajs.274.1.61)
64. Pomar L, Hallock H. 2008 Carbonate factories: a conundrum in sedimentary geology. *Earth-Sci. Rev.* **87**, 134–169. (doi:10.1016/j.earscirev.2007.12.002)
65. Munday PL, Warner RR, Monro K, Pandolfi JM, Marshall DJ. 2013 Predicting evolutionary responses to climate change in the sea. *Ecol. Lett.* **16**, 1488–1500. (doi:10.1111/ele.12185)